Heliyon 7 (2021) e08456

Contents lists available at ScienceDirect

Heliyon

journal homepage: www.cell.com/heliyon

Research article

Synthesis of encapsulated fish oil using whey protein isolate to prevent the oxidative damage and cytotoxicity of titanium dioxide nanoparticles in rats

Mosaad A. Abdel-Wahhab [a,*], Aziza A. El-Nekeety [a], Hagar E. Mohammed [b], Tamer M. El-Messery [c], Mohamed H. Roby [d], Sekena H. Abdel-Aziem [e], Nabila S. Hassan [f]

[a] Food Toxicology & Contaminants Department, National Research Centre, Dokki, Cairo, Egypt
[b] Zoology Department, Faculty of Science, Al-Arish University, Al-Arish, Egypt
[c] Dairy Science Department, National Research Centre, Dokki, Cairo, Egypt
[d] Food Science and Technology Department, Faculty of Agriculture, Fayoum University, Fayoum, Egypt
[e] Cell Biology Department, National Research Centre, Dokki, Cairo, Egypt
[f] Pathology Department, National Research Centre, Dokki, Cairo, Egypt

ARTICLE INFO

Keywords:
Omega-3 fatty acids
Fish oil
Encapsulation
Antioxidant
Oxidative stress
Titanium nanoparticles

ABSTRACT

Fish oil exhibited several beneficial effects on human health; however, its applications face several challenges such as its effects on the organoleptic properties of food and its susceptibility to oxidation. Titanium dioxide NPs (TiO_2-NPs) are utilized widely in pharmaceutical and food applications although there are some reports about their oxidative damage to living organisms. The current work was undertaken to identify fatty acids content in mullet fish oil, encapsulation, and characterization of the oil, and to assess the protective efficiency of the encapsulated mullet fish oil (EMFO) against the oxidative damage and genotoxicity of TiO_2-NPs in rats. Sixty female Sprague-Dawley rats were distributed to 6 groups and treated for 21 days included the control group; TiO_2-NPs-treated group (50 mg/kg b.w); the groups treated with EMFO (50 or 100 mg/kg b.w) and the groups received TiO_2-NPs plus EMFO at the low or high dose. Samples of blood, liver, and kidney were taken for different assays and histological studies. The GC-FID analysis showed that a total of 14 different fatty acids were found in Mullet fish oil included 41.4% polyunsaturated fatty acids (PUFAs), 31.1% monounsaturated fatty acids (MUFAs), and 25.1% saturated fatty acids (SFAs). The structure of EMFO was spherical with an average diameter of 234.5 nm and a zeta potential of -6.24 mV and was stable up to 10 days at 25 °C with EE of 81.08%. The PV of EMFO was decreased at 5 days then increased at 15 days; however, TBARS was increased throughout the storage time over 15 days. The biological evaluation showed that TiO_2-NPs disturb the hepato-nephro functions, lipid profile, inflammatory cytokines, oxidative stress markers, antioxidant enzymes activity, and their corresponding gene expression along with severe pathological alterations in both hepatic and renal tissue. Co-administration of EMFO induced a strong antioxidant role, and the high level could normalize the majority of the parameters tested and the histological picture of the hepatic and renal tissues. These results pointed out that the encapsulation technology enhances the protective role of EMFO against oxidative stress and genotoxicity of TiO_2-NPs through the prevention of ω-3 PUFAs oxidation and controlling their release.

1. Introduction

Omega-3 polyunsaturated fatty acids (ω-3 PUFAs) are long-chain fatty acids (FAs) derived from plants and fish (Hu et al., 2002). ω-3 PUFAs such as docosahexaenoic acid (DHA) and eicosapentaenoic acid (EPA) found in the fish oil exhibited several beneficial effects on the human health including cardioprotective in clinical studies of Eskimos (Endo and Arita 2016; Kromhout et al., 1985), antioxidant (Bouzidi et al., 2010; Carrepeiro et al., 2011), anti-inflammatory (Yang et al., 2013; Ellulu et al., 2015), immunoregulatory (Calviello et al., 2006), anti-tumour (Eltweri et al., 2017), improvement in brain function and neurological development (Kerdiles et al., 2017) and protection against other metabolic and chronic diseases (Saini and Keum 2018; Curioni et al., 2019). However, ω-3 PUFAs are susceptible to the oxidation because they are the first targets of the free radical strike when the oxidation process is initiated (Estévez 2015; Scislowski et al., 2005). The products of lipids

* Corresponding author.
E-mail address: mosaad_abdelwahhab@yahoo.com (M.A. Abdel-Wahhab).

https://doi.org/10.1016/j.heliyon.2021.e08456
Received 30 August 2021; Received in revised form 30 October 2021; Accepted 18 November 2021

oxidation degrade the food quality mainly, texture, flavor, color, and nutritional value affecting certain organs and tissues (Priscilla and Prince 2009). Currently, encapsulation of ω-3 PUFAs has been paid attention to protect ω-3 PUFAs against spontaneous oxidation and deterioration during storage or the processing of food (Chang and Nickerson 2018; Mohammed et al., 2020), improve its water solubility, physicochemical stability, and bioavailability (McClements and Rao 2011; Ningning et al., 2020) and improve their delivery and controlled release (Abdel-Wahhab et al., 2018). Whey protein isolate (WPI) is commonly used as a food emulsifier to promote its ability to form and stabilize oil droplets in emulsions (Singh 2011).

Nanotechnology has witnessed a tremendous expansion of research and potential applications, recent reports have shown its beneficial pharmaceutical and therapeutic uses (Dawood et al., 2018; Zahin et al., 2020). However, it considers as a double-edged sword, where some studies have suggested toxic effects on living organisms (Abdel-Wahhab et al., 2020, 2021; Santonastaso et al., 2019). Titanium dioxide NPs (TiO_2-NPs) are widely utilized in several commercial products such as drugs, cosmetics, food colorants, sunscreens, skincare products, water treatment, varnishes, and paints (Rajh et al., 2014; Winkler et al., 2018) due to their extreme stability, biocompatibility, strong oxidizing properties and photocatalytic properties (Yin et al., 2013). TiO_2-NPs enters the body via different ways such as inhalation, ingestion, medical injections, and skin uptake (Migdal et al., 2010) and probably distribute to the body organs through the circulatory system however its toxicity of varied with particle sizes and exposure conditions. There are three postulated mechanisms for TiO_2-NPs toxicity; apoptosis and oxidative damage induced by their production of ROS, lipid peroxidation, and inducing oxidative DNA damage (Kandeil et al., 2019; Moradi et al., 2019). This study was undertaken to protect ω-3 PUFAs from oxidation through the encapsulation process using WPI and to evaluate their efficiency to counteract the oxidative damage and disturbances in genes expression in rats exposed orally to TiO_2-NPs.

2. Materials and methods

2.1. Materials, chemicals and kits

TiO_2-NPs with a specific surface area of 50 m^2/g, an average diameter of 100 nm, and purity = 99.9%, were purchased from Degussa Corporation (Hanau, Germany). According to the produced company reports, the specific surface area of TiO_2-NPs was determined by BET surface area analyzer (OMNISORP-100CX, Coulter, USA), and particle size was scanned by transmission electron microscopy (JEM200-CX, JEOL, Tokyo). WPI was supplied by Aromse Co. (Turkey). Non-traditional *Nigella sativa* (black seed) oil (BSO) was supplied by the oil extraction unit, National Research Centre (NRC), Egypt. Ammonium thiocyanate, ferrous sulfate, and barium chloride were supplied by Sigma Co. (St. Louis, MO, USA), hydrochloride acid, methanol, and hexane were supplied by SHAM Co. (Germany). Isooctane, 2-propanol, and 1-butanol were obtained from BDH Co. (England). Kits for transaminase (AST & ALT) were provided by Randox, Antrim Co. (UK). Kits for cholesterol (Cho), triglycerides (TG), high-density lipoprotein (HDL), low-density lipoprotein (LDL), creatinine, uric acid, urea, albumin (Alb), total protein (TP), total bilirubin (T.BIL), direct bilirubin (D.BIL) were provided by FAR Diagnostics Co. (Via Fermi, Italy). Kits for nitric oxide (NO), malondialdehyde (MDA), Catalase (CAT), superoxide dismutase (SOD), and glutathione peroxidase (GPx) were supplied by Eagle diagnostics (Dallas, TX, USA). ELISA kit for alpha-fetoprotein (AFP) was supplied by Biochem Immuno Systems Co. (Montreal, Canada). Tumor necrosis factor-alpha (TNF-α) kits were supplied by Orgenium (Helsinki, Finland). Carcinoembryonic antigen (CEA) Kit was supplied by Biodiagnostic Co. (Giza, Egypt). PreMix cDNA and RNase-free DNase kits were supplied by iNtRON Biotechnology Co. (Seoul, Korea). Trizol and DNase kit were supplied by Promega Corporation Co. (WI, USA) and the DNA ladder was supplied by Invitrogen Co. (Massachusetts, USA). Other chemicals utilized in this work were of the highest available analytical grade.

2.2. Extraction of mullet fish (Mugil cephalus) oil (MFO)

Mullet's heads were collected from the waste of local restaurants in Fayoum city, Egypt, and were kept in refrigerator at -20 °C until extracted by enzymatic hydrolysis by using *Bacillus Licheniformis* protease. The fish heads (as the waste parts) were utilized in this study and were identified by Fish Processing and Technology Laboratory, National Institute of Oceanography and Fisheries, Ministry of Scientific Research, Egypt. The enzymatic hydrolysis was conducted at 70 °C in a stirred thermostated reactor (2 L) where raw material (15 kg) was suspended in distilled water. The pH was amended to 7 with 4 M NaOH under mixing for 15 min. The enzymatic solution was added and the reaction was continued for 2 h under nitrogen. The pH was remained steady by automatically adding 4 M NaOH during hydrolysis according to the pH-stat method. The medium was filtered coarsely to retain bones, while the liquid phase was undergone a subsequent centrifugation in order to separate oil and emulsified fractions from the underlying aqueous phase. The enzyme was inactivated in hydrolysate by heat treatment with live steam injection (95 °C, 10 min).

2.3. Determination of fatty acids in mullet fish oil (MFO) by gas chromatography-flame ionization detector (GC-FID)

The determination of fatty acid methyl esters (FAMEs) was conducted as described previously (Ackman 1998) by the transmethylation of the lipid aliquots (100 mg). Each sample was dissolved in hexane (1.5 mL) and 1.5 mL borontrifluoride in methanol (8%, w/vol), and heated for 1 h at 100 °C. After cooling, FAMEs samples were extracted in hexane under nitrogen then were determined by Shimadzu gas chromatography equipped with the flame ionization detector (FID) and a fused-silica capillary column (25 m * 0.25 mm * 0.5 mm; BPX70 SGE Australia Pty Ltd.). The temperature was set as follows: 2 min initial period at 70 °C, then increasing at 40 ° C/min to reach a second step at 180 °C during 8 min and flowing out at 3° C/min to the final period (220 °C, 45 min). Injection and detector ports were maintained at 230 °C and 260 °C, respectively. The identification of fatty acids (FAs) was done by the comparison of the relative retention times with appropriate standard mixtures (PUFA 1 from a marine source and PUFA 2 from an animal source; Supelco, Bellefonte, PA, USA) and an internal standard (C 23:0). The results were displayed as a percentage of the total identified FAs.

2.4. Preparation of MFO nano-emulsion

The wall material was prepared by WPI (10%) in distilled water and stirring for 1 h. A mixture of MFO and NSO (1:1) was added to the wall martial solution at a ratio of 1:4 (wall: core material) then subjected to homogenization using an Ultra-Turrax homogenizer (T18 basic IKA, Wilmington, USA), operating at a speed of 18,000 rpm for 5 min. The coarse emulsion was homogenized by ultrasonication at 160 W powers, 20 kHz frequency, and with 50 % pulse for 20 min. An ultrasound titanium probe with 3.8 nm diameter was used. The samples were placed in cold water bath (4 °C) to prevent the overheating of emulsion.

2.5. Spray drying for capsulation

The resulted emulsion was divided into two portions: the first portion was utilized for determination of encapsulation efficiency and stability; however, the second portion was spray-dried using a laboratory spray dryer (Mini spray dryer B-290, BÜCHI Labortechnik, Switzerland) with a 1.5 mm nozzle diameter and main spray chamber of 500 × 215 mm. A peristaltic pump was used for pumping the emulsion to the dryer at a 5 cm^3/min flow rate and the flow rate of drying air was adjusted at 2.5 m^3/min and pressure of 0.06 MPa. The inlet and outlet air temperatures were

180–195 and 71–75 °C, respectively. The powdered microcapsules were collected and kept in an air-tight desiccator for further characterization.

2.6. Characterization of encapsulated mullet fish oil (EMFO)

2.6.1. Particle size and zeta potential (ζ-potential)

The average diameter, the size distribution, and ζ-potential were determined by using a particle size analyzer (Nano-ZS, Malvern Instruments Ltd., UK). For measuring the ζ-potential, the sample was sonicated for 30–60 min just before assessment, and each sample was assayed in triplicate.

2.6.2. Surface morphology of microcapsules powder

A Scanning Electron Microscopy (Quanta FEG 250 SEM, Tokyo, Japan) was utilized for the determination of the dried microcapsules morphology. The sample was coated with a light gold spray (Sputter coater, Agar Aids, England) for 45 s and were imaged under SEM operates with a low beam current at 7 kV. However, transmission electron microscopy (TEM, JEM-2100 electron microscope) was utilized to observe the graphene on the nanoemulsion surface.

2.6.3. Emulsion stability (ES)

Separation of the serum from the emulsion was taken as an index of ES (Carneiro et al., 2013Carneiro et al., 2013). The emulsion was transferred to a cylinder (20 mL); capped and kept for 24, 48, 72, 96, and 120 h, at 25 °C. The height of the separated serum from the emulsion was monitored as % separation and was calculated using the following Eq. (1):

$$\% \text{ Separation} = H1/H0 \text{ x } 100 \quad (1)$$

where: *H1* is the upper phase height and *H0* is the initial height of emulsion.

2.6.4. Encapsulation efficiency (EE)

The method reported by Bae and Lee (2008) was applied for the determination of EE. Hexane (50 mL) was added to microcapsule powder (1.5 g) in a glass jar and shook for 2 min to extract the free oil. The extract was filtered using a filter paper (Whatman No.1) and the powder collected on the filter was rinsed 3 times with hexane (20 mL), then the combined extracts were evaporated to dryness at 60 °C until their weight become constant which represents the non-encapsulated oil.

EE was calculated using the following Eq. (2):

$$EE = (TO - SO)/TO \text{ x } 100 \quad (2)$$

where: SO and TO are the surface and total oil content, respectively.

2.6.5. Oxidative stability of mullet fish oil emulsion (MFOE)

MFOE samples were incubated in dark at 55 °C for 14 days using an NÜVE incubator (Turkey), and lipid hydroperoxides and TBARS were measured every 2 days (Walker et al., 2015). In brief, MFOE was extracted by the addition of 1.5 ml of mixture of 2-propanol/isooctane (1:3 v/v) to 1 g of sample. The mixture was vortexed for the 30 s, and centrifugation at 1000 xg for 2 min. An aliquot of the top layer was taken and mixed with a volume of 2.8 ml of pre-mixed methanol/1-butanol (2:1 v/v), then 30 μL of ferrous iron solution (3.94 M): ammonium thiocyanate (1:1 v/v) was added. The absorbance was read after 2 min using UV-visible spectrophotometer (BioTek, Synergy HT, USA). To construct the Fe^{3+} calibration curve, a stock of Ferric chloride (10 mg/mL) was diluted with chloroform/methanol (7:3 ratios) to obtain 5–30 mg/L standard Fe^{3+} sample. All samples were read in triplicate.

2.6.6. Thiobarbituric acid-reactive substances (TBARS)

TBARS samples were held in 50 mL disposable centrifuge polypropylene tubes (Fisher Scientific, Pittsburg, PA, USA) in the dark at 55 °C and were read each other day for 14 days (El-Messery et al., 2020). Emulsion (1.0 mL) and 2.0 mL of TBA reagent (15% w/v trichloroacetic acid, 0.375% w/v thiobarbituric acid, and 0.25 M HCl with 2% BHT in ethanol solution) were vortexed in glass test tubes with screw caps. The tubes were incubated for 15 min in a water bath (90 °C) then moved to a room temperature water bath to cool for 10 min. The tubes were centrifuged for 15 min (1000 g) and then sat for 10 more minutes. The supernatant absorption was read at 532 nm. TBARS concentrations were calculated as nM using a standard curve of TEP at concentrations between 0 and 20 nM and all samples were read in triplicate.

2.7. In vivo evaluation

2.7.1. Animals and experimental setup

Sixty sexually mature female Sprague-Dawley rats (3 month-old and 150–160 g body weight) were supplied by the Animal House Colony, NRC, Dokki, Cairo, Egypt. All animals were fed on a standard pellet diet and maintained in filter top polycarbonate cages in a ventilated animal room (12 h dark/light cycle, 25 ± 1 °C and 25–30% humidity) at the Animal House Lab, NRC. Egypt. All animals were received humane care in compliance with the guidelines of the Animal Care and Use Committee of the NRC, Dokki, Cairo, Egypt, and the National Institute of Health (NIH publication 86-23 revised 1985). After an adaptation period of a week, animals were distributed into six groups (10 rats/group) and orally treated by a stomach tube for 21 days as follows: group1; normal control, group 2; rats received an aqueous solution of TiO_2-NPs (50 mg/kg b.w), groups 3 and 4; rats treceived low dose (LD) or high dose (HD) of encapsulated mullet fish oil (EMFO) (50 and 100 mg/kg b.w, respectively), and groups 5 and 6; rats received EMFO (LD) or (HD) plus TiO_2-NPs. The animals were observed daily for any signs of toxicity during the experimental period.

2.7.2. Sampling and tissue preparation

2.7.2.1. Blood samples. On day 21, samples of blood were collected from all animals after being fasted for 12 h via the retro-orbital venous plexus under isoflurane anesthesia. Sera were separated using cooling centrifugation and kept at -20 °C until analysis. The sera were used to determine liver and kidney markers, lipid profile, CEA, AFP, and TNF-α according to the instructions of the kit.

2.7.2.2. Tissue samples

2.7.2.2.1. Assessment of oxidative stress markers. After the collection of blood samples, animals were euthanized and samples of the liver and kidney were collected. A sample from each organ of each experimental animal was weighed, and homogenized in phosphate buffer (pH 7.4) to yield 20% w/v of homogenate according to Lin et al. (1998). The homogenate was centrifuged (1700 rpm, 4 °C and 10 min) then was used for the assay of MDA, NO, GPx, CAT, and SOD.

2.7.2.2.2. Cytogenetic analysis. Freshly collected liver tissues were frozen in the liquid nitrogen and kept in a -80 °C freezer before RNA isolation. Total RNA was isolated from tissue samples using Trizol reagent. The concentration and quality of RNA were determined by NanoDrop™ 1000 Spectrophotometer (Thermo Fisher Scientific, USA), and only the samples of high quality with A260/A280 ratios between 1.8 and 2.2 were used. Reverse transcription-cDNA was stored at 20°C for later use or directly used as a semi-quantitative PCR template. The expression of the selected genes was quantified by using quantitative real-time PCR performed in a One-Step SYBR Select Master Mix Kit as previously described (Kim et al., 2009). The gene-specific primer sequences for GAPDH, GPx, SOD, CAT, Bax, Bcl-2, and TNF-α are shown in Table 1. Real-time quantitative PCR (RT-qPCR) was carried out on Stratagene Mx3005P Real-Time PCR System (Agilent Technologies) in a 20-μL reaction volume using, 1 μL cDNA, 10 μM of forward and reverse primers, 10 μL TOPreal™ qPCR 2× PreMIX (SYBR Green with low ROX) (Enzynomics) and DNAse-free water. Each sample was amplified in a

Table 1. Details giving primer sequences for the genes amplified.

cDNA	Accession number	Forward primer	Reverse primer	RT-PCR product size
GAPDH	NM_017008.4	CAAGGTCATCCATGACAACTTTG	GTCCACCACCCTGTTGCTGTAG	496
Cu–Zn SOD	FQ210282.1	GCAGAAGGCAAGCGGTGAAC	TAGCAGGACAGCAGATGAGT	477
GPx	NM_030826.4	CTCTCCGCGGTGGCACAGT	CCACCACCGGGTCGGACATAC	290
CAT	NM_012520.2	GCGAATGGAGAGGCAGTGTAC	GAGTGACGTTGTCTTCATTAGCACTG	652
Bax	NM_017059.2	AGGATGATTGCTGATGTGGATAC	CACAAAGATGGTCACTGTCTGC	300
Bcl-2	NM_016993.2	GCTACGAGTGGGATACTGGAGA	AGTCATCCACAGAGCGATGTT	446
TNF-α	NM_012675.3	CCACCACGCTCTTCTGTCTAC	ACCACCAGTTGGTTGTCTTTG	256

minimum of triplicates. Amplification was performed with a 15-min denaturation at 95 °C, then 40 cycles of 95 °C for 12 s, 56–63 °C for 15 s, and 72 °C for 30 s. The expression levels were calculated from the PCR cycle number (C_T) where the increased fluorescence curve passes across a threshold value. The relative expression of target genes was obtained using the comparative C_T ($\Delta\Delta C_T$) method. The ΔC_T was calculated by subtracting β-actin C_T from that of the target gene whereas $\Delta\Delta C_T$ was obtained by subtracting the ΔC_T of the calibrator from that of the test sample. The $2^{-\Delta\Delta CT}$ formula was used for the calculation of relative expression (Pfaffl 2001; Abdel-Wahhab et al., 2021a).

2.7.3. Histological studies

The samples of liver and kidney from each animal were fixed in 10% neutral formalin and paraffin-embedded. Sections (5 μm thickness) were stained with hematoxylin and eosin (H & E) for the histological examination (Bancroft et al., 1996).

2.8. Statistical analysis

Data were expressed as mean ± SE and were statistical analyses using one-way ANOVA. Duncan-test was used as post-hoc using SPSS for Windows (version 2; SPSS Inc., Chicago, IL, USA). The significance of differences among means was determined at $p \leq 0.05$.

3. Results

3.1. Fatty acids analysis in MFO

The GC-FID chromatogram (Figure 1) and the analysis of the fatty acids (Table 2) of MFO indicated the identification of 14 fatty acids with the percentage of 41.1, 31.1, and 25.1% of polyunsaturated fatty acids (PUFA), monounsaturated fatty acids (MUFAs) and saturated fatty acid (SFA), respectively.

Table 2. Fatty acid composition of Mullet oil.

No	Fatty acid	Name of Fatty acid	Content (area %)
1	C14:0	Myristic acid	7.3 ± 0.65
2	C16:0	Palmitic acid	14.6 ± 0.43
3	C16:1	Palmitoleic acid	8.5 ± 0.35
4	C18:0	Stearic acid	3.2 ± 0.02
5	C18:1 n-9	Oleic acid	15.8 ± 0.59
6	C18:2–6	Linoleic acid	5.1 ± 0.34
7	C18:3 n-3	Linolenic acid	2.3 ± 0.94
8	C18:4 n-3	Stearidonic acid	1.4 ± 0.68
8	C20:1 n-9	Eicosenoic acid	6.9 ± 0.16
10	C20:4 n-6	Arachidonic acid	9.6 ± 0.31
11	C20:4 n-3	Dihomo-γ-linolenic acid	1.5 ± 0.78
12	C20:5 n-3	Eicosapentaenoic acid	3.8 ± 0.06
13	C22:5 n-3	Docosapentaenoic acid	6.3 ± 0.43
14	C22:6 n-3	Docosahexaenoic acid	11.5 ± 0.31
	∑ SFA	25.1	25.1
	∑ MUFA	31.1	31.1
	∑ PUFA	41.4	41.4

All values are mean of three replicates ±standard deviation.
SFA, saturated fatty acid; MUFA, monounsaturated fatty acid; PUFA, polyunsaturated fatty acid.

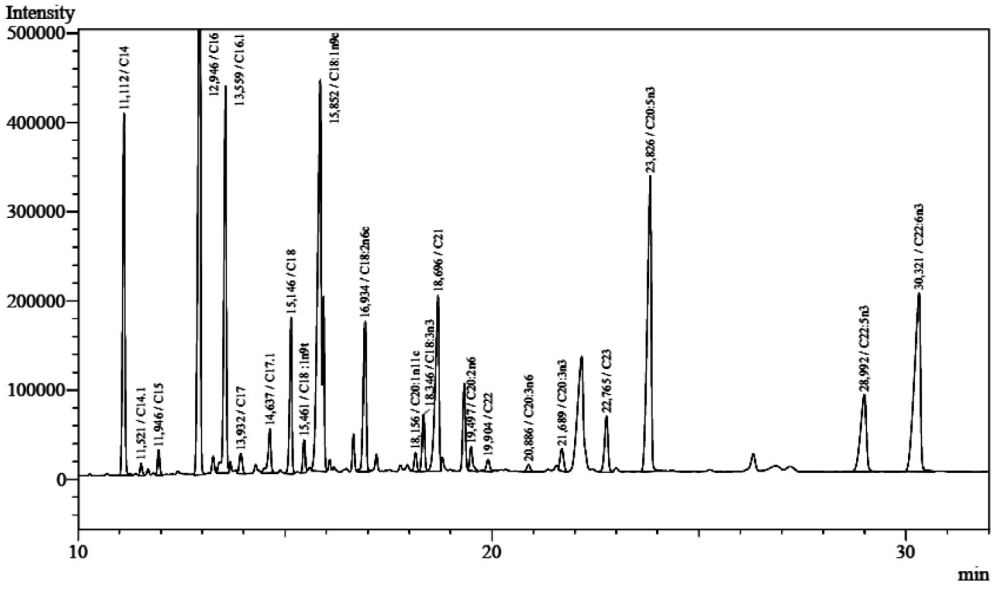

Figure 1. GC chromatograms for mullet fish oil analysis.

3.2. Characterization of emulsion

The present results showed that the emulsion was stable up to 10 days at 25 °C since the separation % after 10 days/25 °C was 08.00 ± 0.98. The mean diameter (D32) was 234.50 ± 1.03 nm and ζ-potential were -06.24 ± 0.56 mV. The SEM image showed that the microcapsules were mostly spherical structures (Figure 2) with some indentations and small wrinkles on their surfaces. The results also showed the preparation of EMFO using spray drying resulted in EE of 81.08 ± 0.47%.

3.3. PV and TBARs

PV and TBARS (Table 3) of EMFO showed a decrease in PV after a storage period of 5 days then it was increased dramatically at 15 days as lipid oxidation proceeded. Moreover, TBARS was also increased by the storage period throughout 15 days.

3.4. In vivo results

The biological evaluation revealed that TiO_2-NPs induced toxicity and disturbed the biochemical indicators in animals that received TiO_2-NPs alone. This toxicity was primarily manifested by the remarkable decrease in body weight (Figure 3). Animals received EMFO at the low or the high doses were comparable to the untreated control. Moreover, the body weight of the groups that received TiO_2-NPs plus EMFO (LD) or EMFO (HD) was improved significantly and was comparable to the untreated control animals by the termination of the experiment period.

The effect of EMFO on the serum indicators in rats that received TiO_2-NPs is depicted in Table 4. TiO_2-NPs administration caused a significant increase in ALT, AST, T.BIL, D.BIL, creatinine, urea, and uric acid accompanied by a significant decrease in TP and Alb. The low dose of EMFO did not amend any of these parameters except creatinine which was lower than the control. However, administration of EMFO (HD) decreased D.BIL and creatinine and increased urea but did not change the other parameters when compared with the untreated control rats. Animals that received EMFO (LD) or (HD) plus TiO_2-NPs showed a significant improvement in all the biochemical indicators and EMFO (HD) could normalize ALT, AST, and T.BIL.

Administration of TiO_2-NPs disturbs the lipid profile as manifested by the remarkable increase in Cho, TG, and LDL-Cho and the decrease in HDL-Cho compared with those in the control group (Table 5). No significant difference was noticed in lipid profile between animals who received EMFO (LD) and the control; however, TG, LDL-Cho were decreased and HDL-Cho was increased in the group that received EMFO (HD) but an insignificant change was observed in Cho level in this group. Additionally, the levels of Cho and LDL-Cho in the groups that received TiO_2-NPs plus EMFO at both doses were within the normal range of the untreated control animals and the levels of TG and HDL-Cho were significantly improved in these groups (Table 5). The data shown in Table 6 showed a remarkable increase in CEA, AFP, and TNF-α in the group that received TiO_2-NPs compared to those in the untreated control group. Administration of EMFO alone at both dose levels did not cause any significant changes in these parameters. Moreover, the co-administration of EMFO (LD) or (HD) plus TiO_2-NPs improved these cytokines and the high dose of EMFO could normalize TNF-α.

Table 3. PV and TBARS of EMFO during storage period.

Storage (Days)	PV	TBARS
0	20.97 ± 2.71	1.06 ± 0.08
5	19.02 ± 8.17	1.18 ± 0.02
10	52.65 ± 2.21	1.37 ± 0.03
15	51.23 ± 4.21	1.71 ± 0.08

Data are expressed as the mean value ±SE (n = 3).

Administration of TiO_2-NPs disturbed the activity of antioxidant enzymes in the liver and kidney (Table 7). Treatment with TiO_2-NPs alone decreased the hepatic and renal CAT, SOD and GPx; however, EMFO (LD) alone increased renal CAT and GPx but no remarkable effect was observed in renal SOD or hepatic CAT, SOD, and GPx. Moreover, EMFO (HD) increased GPx in the liver, CAT, and GPx in the kidney but no remarkable change was observed in renal SOD or hepatic CAT and SOD. Co-administration of TiO_2-NPs and EMFO (LD) or (HD) improved the hepatic and renal antioxidant enzymes activity and this improvement was more pronounced in the group received TiO_2-NPs plus EMFO (HD) which normalized renal CAT and GPx.

The results presented in Table 8 illustrated that administration of TIO_2-NPs increased renal and hepatic MDA and NO. EMFO (LD) or (HD) decreased the hepatic MDA and NO in a dose-dependent without any significant changes in these indicators in the kidney tissue. Furthermore, treatment with TiO_2-NPs plus EMFO (LD) or (HD) improved significantly the hepatic and renal MDA, and NO and EMFO (HD) could normalize MDA in both organs.

3.5. Apoptotic genes expression

The changes in hepatic mRNA gene expression of pro-apoptotic Bax (Figure 4A), TNF-α (Figure 4B), and antiapoptotic Bcl-2 (Figure 3C) in the treated groups as compared with the controls and the housekeeping glyceraldehyde-3-phosphate dehydrogenase gene (GAPDH) showed that TiO_2-NPs alone enhanced Bax and TNF-α mRNA expression and suppresses Bcl-2 mRNA expression. However Bax, Bcl-2 and TNF-α mRNA expression in the animals that received EMFO (LD or HD) did not show any significant difference from the control animals. Co-treatment of TiO_2-NPs plus EMFO remarkably improves the levels of transcription of these genes.

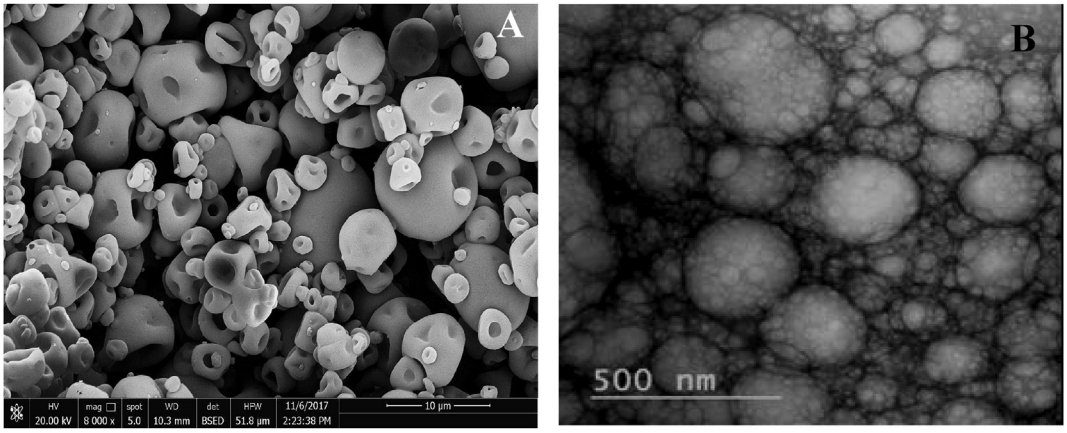

Figure 2. SEM (A) and TEM (B) image of spray-dried nanoemulsions of EMFO (8000x).

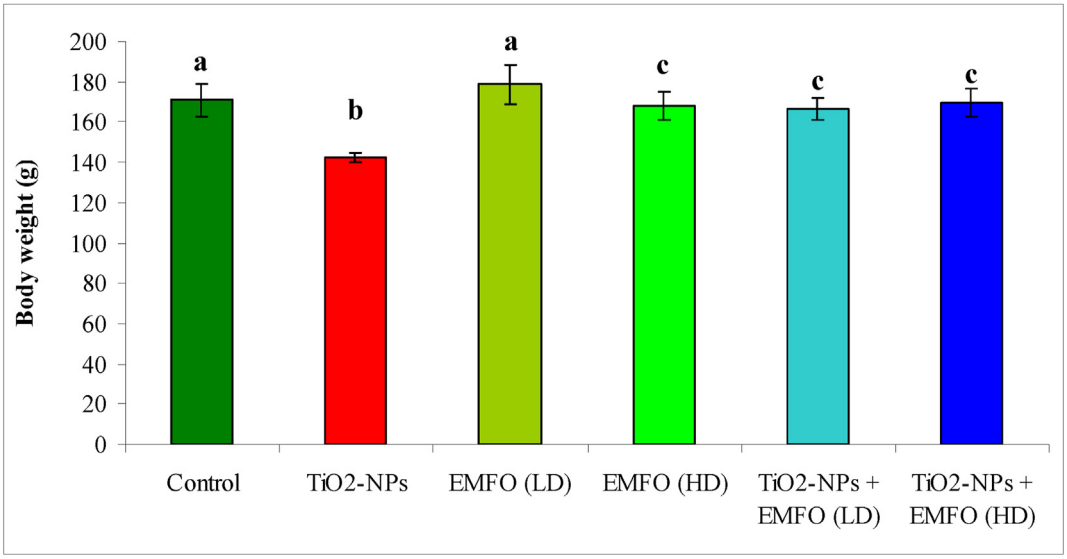

Figure 3. Effect of EMFO on body weight in rats treated with TiO_2-NPs. Columns superscripts with different letters are significantly different ($P < 0.05$).

Table 4. Effects of EMFO on serum biochemical parameters in rats treated with TiO_2-NPs.

Groups Parameter	Control	TiO_2-NPs	EMFO (LD)	EMFO (HD)	TiO_2-NPs + EMFO (LD)	TiO_2-NPs + EMFO (HD)
ALT (U/L)	44.67 ± 5.17^{a}	82.33 ± 5.93^{b}	45.00 ± 2.65^{a}	45.33 ± 1.45^{a}	51.67 ± 2.85^{c}	46.67 ± 6.32^{a}
AST (U/L)	152.67 ± 3.48^{a}	205.00 ± 6.24^{b}	148.33 ± 3.18^{a}	152.67 ± 3.48^{a}	183.00 ± 3.21^{c}	153.00 ± 3.61^{a}
Alb (mg/dl)	2.74 ± 0.11^{a}	1.77 ± 0.05^{b}	2.38 ± 0.21^{ac}	2.61 ± 0.11^{a}	2.53 ± 0.28^{c}	2.50 ± 0.03^{c}
TP (g/dl)	6.48 ± 0.21^{a}	4.80 ± 0.53^{b}	6.45 ± 0.14^{a}	6.47 ± 0.18^{a}	5.94 ± 0.45^{d}	5.98 ± 0.07^{d}
T. BIL (mg/dl)	0.09 ± 0.01^{a}	0.87 ± 0.06^{b}	0.09 ± 0.01^{a}	0.09 ± 0.01^{a}	0.14 ± 0.01^{c}	0.09 ± 0.01^{a}
D. BIL (mg/dl)	0.03 ± 0.01^{a}	0.06 ± 0.01^{b}	0.03 ± 0.01^{a}	0.02 ± 0.01^{c}	0.04 ± 0.02^{d}	0.02 ± 0.01^{c}
Creatinine (mg/dl)	0.81 ± 0.06^{a}	1.30 ± 0.04^{b}	0.70 ± 0.04^{c}	0.66 ± 0.04^{d}	0.94 ± 0.02^{e}	0.88 ± 0.01^{f}
Urea (mg/dl)	49.67 ± 4.48^{a}	70.33 ± 0.88^{b}	49.33 ± 5.24^{a}	57.00 ± 1.15^{c}	65.33 ± 1.67^{c}	52.00 ± 2.00^{d}
Uric acid (mg/dl)	1.26 ± 0.17^{a}	2.53 ± 0.30^{b}	1.28 ± 0.05^{a}	1.12 ± 0.08^{a}	1.44 ± 0.07^{c}	1.46 ± 0.22^{c}

Within each row, means superscripts with different letters are significantly different ($P < 0.05$).

Table 5. Effects of EMFO on lipid profile parameters in rats treated with TiO_2-NPs.

Groups parameter	Control	TiO2-NPs	EMFO (LD)	EMFO (HD)	TiO2-NPs + EMFO (LD)	TiO2-NPs + EMFO (HD)
Cho (mg/dl)	64.33 ± 2.96^{a}	84.67 ± 1.20^{B}	66.67 ± 6.17^{a}	62.00 ± 1.00^{a}	65.67 ± 2.91^{a}	54.67 ± 3.71^{a}
TG (mg/dl)	79.21 ± 1.37^{a}	96.44 ± 2.34^{b}	76.67 ± 3.28^{a}	73.33 ± 2.96^{c}	84.67 ± 1.45^{d}	81.00 ± 2.31^{d}
LDL-Cho (mg/dl)	27.38 ± 2.52^{a}	38.15 ± 2.88^{b}	26.67 ± 1.86^{a}	24.33 ± 0.88^{c}	26.67 ± 1.20^{a}	26.87 ± 2.83^{a}
HDL-Cho (mg/dl)	34.27 ± 1.34^{a}	22.67 ± 1.26^{b}	36.33 ± 1.67^{a}	41.28 ± 2.77^{d}	28.84 ± 2.64^{e}	31.38 ± 1.62^{f}

Within each row, means superscripts with different letters are significantly different ($P < 0.05$).

Table 6. Effects of EMFO on serum cytokines in rats treated with TiO_2-NPs.

Parameter Groups	Control	TiO_2-NPs	EMFO (LD)	EMFO (HD)	TiO_2-NPs + EMFO (LD)	TiO_2-NPs + EMFO (HD)
AFP (ng/mL)	0.03 ± 0.002^{a}	0.51 ± 0.02^{b}	0.03 ± 0.001^{a}	0.03 ± 0.01^{a}	0.31 ± 0.02^{c}	0.08 ± 0.003^{d}
TNF-α (ng/mL)	0.36 ± 0.03^{a}	0.57 ± 0.02^{b}	0.35 ± 0.01^{a}	0.36 ± 0.01^{a}	0.41 ± 0.02^{c}	0.37 ± 0.02^{a}
CEA (ng/mL)	2.88 ± 0.45^{a}	5.32 ± 1.14^{b}	2.86 ± 0.22^{a}	2.82 ± 0.22^{a}	2.65 ± 0.34^{c}	2.55 ± 0.51^{c}

Within each row, means superscripts with different letters are significantly different ($P < 0.05$).

Table 7. Effects of EMFO on hepatic and renal antioxidant enzymes in rats treated with TiO_2-NPs.

Parameter Groups	Liver			Kidney		
	CAT (mU/g)	SOD (U/mg)	GPx (U/mg)	CAT (mU/g)	SOD (U/mg)	GPx (U/mg)
Control	7.38 ± 1.33^{a}	3.87 ± 0.56^{a}	35.8 ± 0.50^{a}	6.74 ± 1.32^{a}	2.80 ± 0.03^{a}	23.05 ± 0.58^{a}
TiO2-NPs	3.28 ± 0.84^{b}	1.87 ± 0.66^{b}	24.3 ± 0.17^{b}	3.67 ± 0.57^{b}	1.31 ± 0.17^{b}	19.21 ± 0.58^{b}
EMFO (LD)	7.70 ± 0.24^{a}	3.87 ± 0.1^{a}	32.4 ± 2.31^{a}	7.35 ± 0.12^{c}	2.84 ± 0.01^{a}	26.07 ± 0.28^{c}
EMFO (HD)	7.84 ± 0.14^{a}	4.08 ± 0.02^{a}	39.0 ± 0.03^{c}	7.58 ± 0.22^{c}	2.88 ± 0.07^{a}	29.93 ± 0.24^{d}
TiO2-NPs + EMFO (LD)	5.37 ± 0.05^{c}	2.78 ± 0.09^{c}	28.0 ± 0.07^{d}	5.54 ± 0.14^{d}	1.77 ± 0.04^{c}	21.28 ± 0.70^{e}
TiO2-NPs + EMFO (HD)	5.42 ± 0.05^{c}	3.47 ± 0.26^{d}	29.3 ± 0.03^{d}	6.44 ± 0.60^{a}	1.84 ± 0.01^{d}	23.21 ± 0.68^{a}

Within each column, means superscripts with different letters are significantly different ($P < 0.05$).

3.6. Antioxidant gene expression

The genetic analysis revealed significant changes in mRNA gene expression of hepatic antioxidant enzymes. Administration of TiO_2-NPs markedly suppressed mRNA expression of GPx (Figure 5A), SOD (Figure 5B) and CAT (Figure 5C) compared to the control animals.

Table 8. Effect of EMFO on MDA and NO in liver and kidney of rats treated with TiO_2-NPs.

Parameter Groups	Liver		Kidney	
	MDA (nmol/g)	NO (μmol/g)	MDA (μmol/g)	NO (nmol/g)
Control	144.61 ± 9.66[a]	541.38 ± 9.47[a]	231.85 ± 6.55[a]	768.85 ± 9.82[a]
TiO2-NPs	198.89 ± 10.33[b]	895.87 ± 11.38[b]	299.37 ± 5.58[b]	958.87 ± 10.83[b]
EMFO (LD)	126.74 ± 4.17[c]	533.14 ± 6.67[c]	225.52 ± 5.75[a]	758.57 ± 8.22[a]
EMFO (HD)	117.48 ± 5.35[d]	528.36 ± 4.95[c]	225.52 ± 5.75[a]	749.11 ± 7.64[a]
TiO2-NPs + EMFO (LD)	162.57 ± 6.37[e]	735.84 ± 5.17[d]	261.54 ± 2.31[c]	844.58 ± 5.87[c]
TiO2-NPs + EMFO (HD)	153.81 ± 7.31[a]	636.82 ± 6.14[e]	246.79 ± 9.24[a]	821.64 ± 7.34[d]

Treatment with EMFO (LD or HD) alone increased the expression of mRNA of these antioxidant enzymes. Co-administration of the EMFO plus TiO_2-NPs improved the mRNA expression of these antioxidant genes in a dose-dependent however; these values were still differing significantly than the control animals (Figure 5).

3.7. Histological examination

The examination of control liver sections showed normal hepatocytes structure (Figure 6A). The liver of rats who received EMFO (LD or HD) alone showed normal hepatic lobules with hepatocytes radiating from a central vein and prominent portal area (Figure 6B). The liver of animals that received TiO_2-NPs showed pathological alterations in the portal areas, where, the portal vein showed dilatation with thick wall, congestion, and periportal necrosis. The bile ducts were proliferated and surrounded by aggregation of mononuclear cellular infiltration and fibrous tissues (Figure 6C). However, the liver of animals received TiO_2-NPs plus EMFO (LD) or EMFO (HD) showed normal hepatic lobules with hepatocytes radiating from the central vein and prominent portal area (Figure 6D). The examination of control kidney sections showed normal renal tubules and glomeruli (Figure 7A). The kidney sections of EMFO (LD or HD)-treated rats showed normal tubules and segmented glomeruli (Figure 7B). The kidney sections of rats received TiO_2-NPs showed damaged tubules with pyknotic nuclei and cloudy swelling in the epithelial cells with segmentation and shrinkage of the glomeruli (Figure 7C). The kidney sections of TiO_2-NPs plus EMFO (LD) or EMFO (HD) groups showed more or less normal structure in most renal tubules, but focal necrosis and cloudy swelling are present and the glomeruli are expanded (Figure 7D).

4. Discussion

The GC-FID analysis of MFO indicated the presence of 14 fatty acids included 41.4% polyunsaturated and 41.1% monounsaturated fatty acids besides 25.1% saturated fatty acids. A previous report showed that fish oil is rich in ω-3 PUFAs mainly docosahexaenoic fatty acid (Bratu et al., 2013). These results also indicated that MFO is rich in ω 3 (26.8%), ω 6 (14.7%), and ω 9 (22.7%) fatty acids. Similar results were reported in samples of seven fish oils (catfish, mackerel, salmon, code liver, two species of phytophagous fish, and bream) which indicated that these oils are rich in ω 3, ω 6 and ω 9 fatty acids (Pandiangan et al., 2018).

The external morphology of EMFO showed a spherical shape, various sizes, and apparent cracks or fissures. It is important since no crack appeared that these capsules have low gas permeability with increased protection and retention of active ingredients. Moreover, the variety in size is a typical characteristic of particles produced by spray-drying (El-Messery et al., 2020). The results of emulsion stability showed that EMFO was stable up to 10 days at 25 °C which are in agreement with those reported by Abdel-Razek et al. (2018). The stability of the emulsion is affected by several factors including ζ-potential, the isoelectric point of WPI, and pH (Hu et al., 2003). The negative charge of the EMFO reported herein may increase the dispersion of the emulsion droplet and explain the stability of the emulsion (Cansell et al., 2003; McClements, 2005). Moreover, the D_{32} mean diameter of the emulsion droplets in the current study (234.5 nm) using the ratio of 1:4 core: wall. In this concern, McClements (2005) and Goula and Adamopoulos (2012) reported that the mean droplet size is increased as the ratio of core/wall material increased. However, a previous study showed that the majority of emulsions were kinetically stable for 120 h after their homogenization (Carneiro et al., 2013).

Generally, small emulsion droplets will enclose and embed oils more efficiently within the wall of the microcapsules and intern more stable microcapsules during the spray drying encapsulation process (Goula and Adamopoulos, 2012). Moreover, the poor EE cannot be attributed only to low surface gelling density, but it is also caused partly by the unstable emulsion and the large size of the oil droplet (Badr et al., 2019). Additionally, the changes in PV and TBARS during the storage period

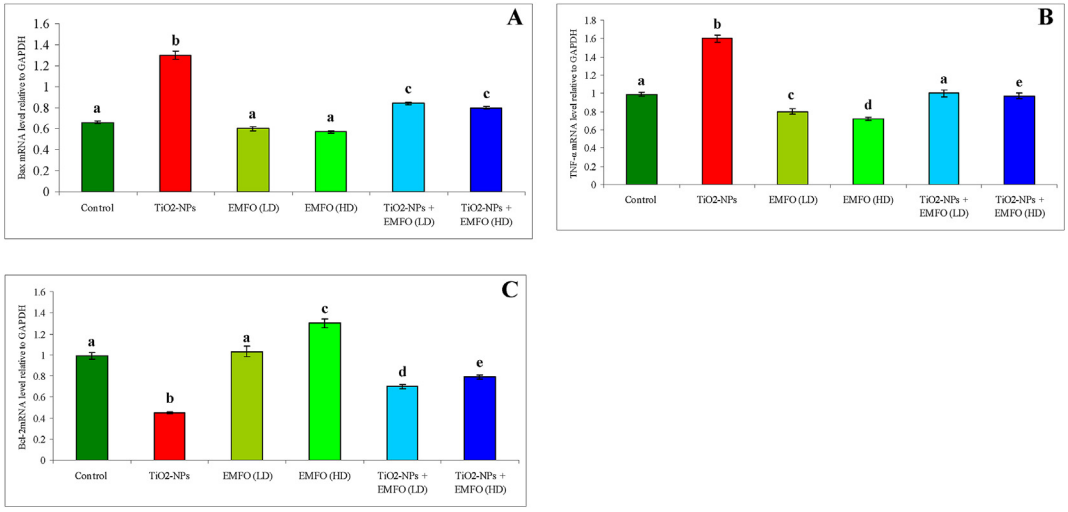

Figure 4. Effect of EMFO on (A) Bax, (B) TNF-α and (C) Bcl-2 gene expression level in liver of rats treated with TiO_2-NPs. The results illustrated are normalized to the level of GAPDH level and the data are the mean of intensity for each gene divided by that for GAPDH. Columns superscripts with different letters are significantly different ($P < 0.05$).

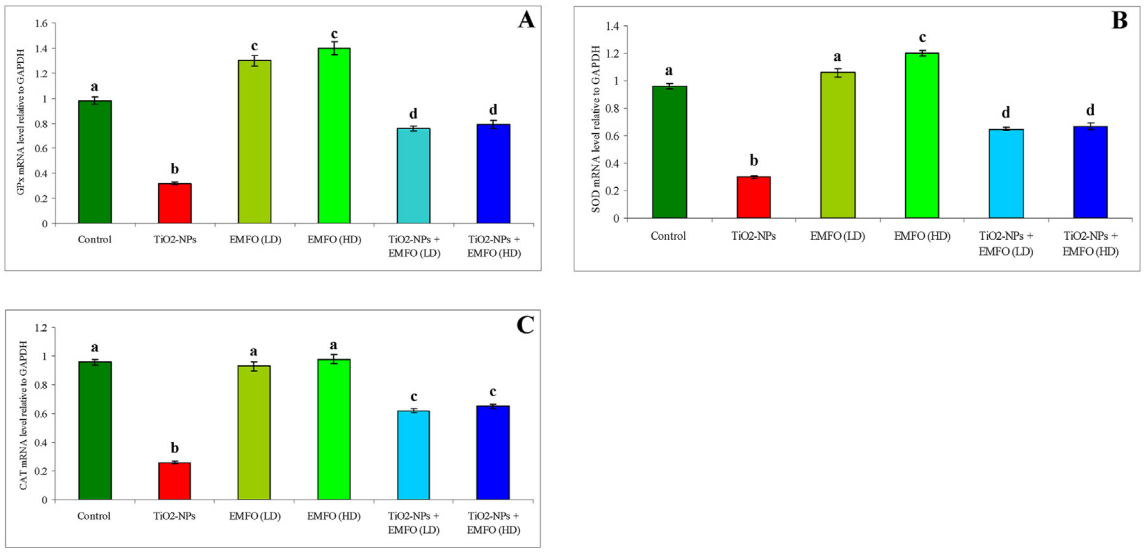

Figure 5. Effect of EMFO on (A) GPx, (B), SOD and (C) CAT mRNA gene expression in the liver of rats treated with TiO_2-NPs. The results illustrated are normalized to the level of GAPDH level and the data are the mean of intensity for each gene divided by that for GAPDH. Columns superscripts with different letters are significantly different ($P < 0.05$).

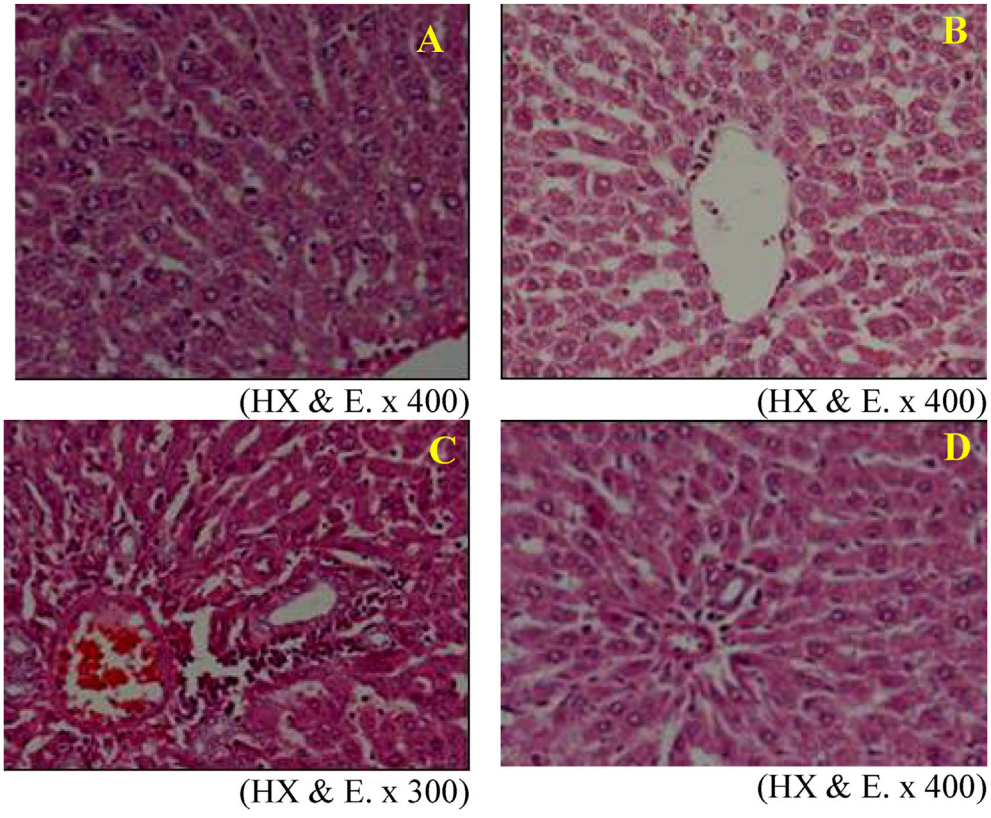

Figure 6. Photomicrographs of liver sections of (A) control rats showing normal hepatocytes structure, (B) rats treated with EMFO (LD) or EMFO (HD) showing normal hepatic lobules with hepatocytes radiating from central vein and prominent portal area. Binucleated hepatocytes are seen, (C) rats treated with TiO_2-NPs showing histological changes in the portal areas, where, the portal vein show dilatation with thick wall, congestion and periportal necrosis. Proliferation in the bile ducts surrounded by aggregation of mononuclear cellular infiltration and fibrous tissues and (D) rats treated with TiO_2-NPs plus FMFO (LD) or FMFO (HD) showing normal hepatic lobules with hepatocytes radiating from central vein and prominent portal area.

suggested that WPI used for the emulsion preparation maybe enhance the ability to bind transition metal ions either in the water phase or at the interface (Elias et al., 2008; Horn et al., 2012).

The application of TiO_2-NPs in the medicine and food sector has been increased dramatically in the manufacture of cheeses, sauces, ice cream, food colorants, confectionery application, and nutritional supplements (Baranowska-Wójcik et al., 2020; Peters et al., 2014). The estimated daily intake of TiO_2-NPs is high especially in children compared with adults due to their dietary habits (Weir et al., 2012). Although there are many published reports describing the toxic hazards of TiO_2-NPs, some findings are still inconsistent (Skocaj et al., 2011; Shakeel et al., 2016a). TiO_2-NPs absorption through the GIT resulted in the toxicity to different organs such as serum, kidney, liver, seminal vesicle, and testes (Bu et al., 2010). In the biological evaluation, the dose of TiO_2-NPs was selected based on the previous work of Shakeel et al. (2016); *however, the dose of EMFO was based on the work of* El-Gendy et al. (2021).

In this study, animals that received TiO_2-NPs exhibited a notable reduction in body weight. Previous reports pointed out that

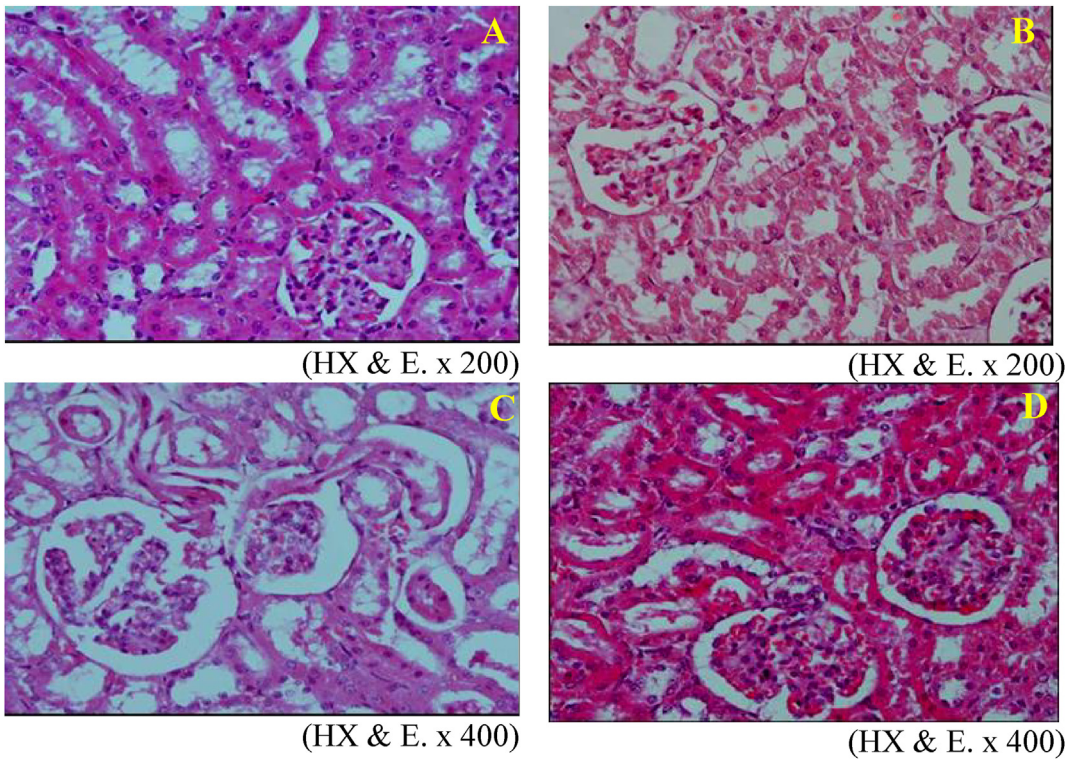

Figure 7. Photomicrographs of kidney sections of (A) control rat showing the renal tubules and glomeruli, (B) rats treated with EMFO (LD) or EFMO (HD) showing the normal tubules and segmented glomeruli, (C) rats treated with TiO_2-NPs showing damaged tubules with pyknotic nuclei and cloudy swelling in the epithelial cells (arrow) and the glomeruli showing segmentation and shrinkage, (D) rat treated with TiO_2-NPs plus EMFO (LD) or EMFO (HD) showing more or less normal structure in most of renal tubules, but focal necrosis and cloudy swelling are present and glomeruli are expanded.

administration of NPs resulted in the shortage of macro and microelements in the body through their effect on the digestion and/or absorption of the food components and led to the reduction of body weight of animals (McClements et al., 2016). Moreover, administration of TiO_2-NPs was reported to induce loss of the appetite leading to the decrease in body weight in mice (Chen et al., 2009) and also decrease the number of intestine villi, reduce the surface which is responsible for nutrients absorption leading to body weight loss and malnutrition (Duan et al., 2010). Additionally, TiO_2-NPs may penetrate the intestinal mucosa resulting in the damage or the chronic failure of intestinal epithelium tissue (Abdel-Wahhab et al., 2021; Ammendolia et al., 2017; Brun et al., 2014).

The results also clearly indicated that administration of TiO_2-NPs disturb the liver and kidney function as they increased the biochemical indices of these organs. It is well known that transaminases are located in the hepatocytes and they release into the serum when these hepatocytes are damaged or injured (Dambach et al., 2005; Thapa and Walia 2007; Mohammed and Safwat 2020). Moreover, animals that received TiO_2-NPs exhibited a marked elevation in urea, creatinine and uric acid suggested kidney injury or dysfunction (Abdelhalim and Jarrar 2011; Fartkhooni et al., 2016). The elevation in LDL, Cho, and TG along with the decrease in HDL in the group treated with TiO_2-NPs suggested that these nanoparticles affected the metabolism of lipid probably via their effect on the lipoprotein lipase enzyme and/or their ability to remove or transfer lipid fractions (Ani et al., 2008; Duan et al., 2010). The elevation of Cho and TG is linked with cardiovascular disease and/or other metabolic syndromes and the disturbances in these indicators has a close relationship with arteriosclerosis; thus, TiO_2-NPs may be considered a causative agent for cardiovascular disorders as suggested in previous reports (Antoni et al., 2018; Chen et al., 2015, 2020; Hong et al., 2017; Reiner 2017).

Animals treated with TiO_2-NPs also showed a significant increase in serum cytokines suggested that these nanoparticles induced inflammatory response via the generation of ROS that reduces the viability of cells and enhances the cytotoxicity through the apoptosis process (Müller et al., 2010; Salman et al., 2021). These results also suggested that the chemistry of TiO_2-NPs surface is responsible for their toxicity and increases TNF-α release and neutrophil-attracting chemokines in a time and size-dependent (Iavicoli et al., 2011; Wu and Tang 2018).

As reported in the literature, oxidative stress is the prime mechanism of TiO_2-NPs toxicity and these particles were reported to encourage ROS formation (Foroozandeh and Aziz 2015). This ROS causes injury to the macromolecules especially lipids, nucleic acids (mainly DNA), carbohydrates, and proteins (Abdel-Wahhab et al. 2020, 2021a; Shukla et al., 2014). The peroxidation of lipids disturbs the cell membrane structure and hence, it causes disturbances in the pivotal cell functions (Rikans and Hornbrook 1997). Reeves et al. (2008) reported that generation of •OH (hydroxyl radical) is the causative factor in TiO_2-NPs-induced oxidative damage as a result of lipids disturbances and MDA accumulation along with the decrease in hepatic antioxidant enzymes (Rajapakse et al., 2012) mainly glutathione (Federici et al., 2007). The decrease in GPx, CAT, and SOD and the elevation of MDA and NO in the liver and kidney reported herein indicated that TiO_2-NPs disturb redox balance leading to oxidative damage (Chen et al., 2020). The high ROS generation reflexes DAN damage and up-regulates 8-OHdG (8-hydroxyl deoxyguanosine) in the liver and kidney (Trouiller et al., 2009). Moreover, reducing the activity of antioxidant enzymes and elevation of MDA may be responsible for cell apoptosis (Abdel-Wahhab et al., 2021; Salman et al., 2021). Additionally, the high level of ROS increases Nrf2, the master regulator for various antioxidant genes expression and Nrf2 deficiency encourages further DNA damage and enhances cancer risk (Shi et al., 2015). Furthermore, the decrease of SOD leads to H_2O_2 (hydrogen peroxide) accumulation in hepatic and renal tissue and in turn inhibit CAT activity (Latchoumycandane and Mathur 2002) which converts the harmful byproduct

of H_2O_2 to O_2 and H_2O to protect the tissues and cells from damage (Sharma et al., 2014).

To explore the probable mechanisms of liver injury in TiO_2-NPs-treated animals, the gene expression assay was conducted as a rapid and quick biomarker (Li et al., 2017). Animals that received TiO_2-NPs showed considerable down-regulation of hepatic SOD, GPx, CAT, and Bcl-2 mRNA expression accompanied by a remarkable up-regulation of TNF-α and Bcl-2 mRNA. These results were harmonized with our biochemical results and confirmed the assumption that these nanoparticles stimulate oxidative damage through the exhaustion of these antioxidant enzymes by suppressing their corresponding gene expression (Abdel-Wahhab et al., 2021; Salman et al., 2021). It is well documented that Bcl-2 is an anti-apoptosis protein responsible for the control of mitochondrial integrity surface, whereas Bax is a pro-apoptotic protein and the balance of these proteins is critical for the control of the sensitivity of the cell to apoptotic stimulations (Ilani et al., 2018). Furthermore, the presence of Bcl-2 on the mitochondrial surface prevents cytochrome c release in the plasma; while Bax protein enhances cytochrome c leakage via the punching of mitochondrial membrane holes (Kroemer et al., 2007). Also, the imbalance in Bax: Bcl-2 ratio activates the caspase-dependent apoptotic pathway as suggested by Peng et al. (2016). These results pointed out that ROS generation in TiO_2-NPs-exposed animals affects the mitochondrial membrane potential as a consequence of apoptosis as suggested in previous studies (Abdel-Wahhab et al., 2020; Zhao et al., 2009). The up-regulated of hepatic TNF-α mRNA in TiO_2-NPs-treated animals revealed the inflammatory response and harmonized with the literature (Chen et al., 2015; Trouiller et al., 2009).

The pathological examination of the hepatic and renal sections reported herein indicated that administration of TiO_2-NPs resulted in severe histological changes in these organs and accommodated with the literature (Abdel-Wahhab et al., 2021; Morgan et al., 2018). Similar observations were reported by Valentini et al. (2019) who found pathological alterations in liver sections which were primarily related to oxidative damage and the most changes were localized nearby the central vein. Additionally, the kidney sections showed damage in the tubules with pyknotic nuclei and cloudy swelling in the epithelial cells and the glomeruli showed segmentation and shrinkage. These findings were similar to those reported in the literature of TiO_2-NPs toxicity (Abdel-Wahhab et al., 2021; Epstein 1997; Salman et al., 2021).

It is now accepted that the toxicity of TiO_2-NPs is mainly due to ROS generation and the induction of oxidative stress. Several reports suggested that fish oil supplementation possess various health beneficial activities such as the suppression of the oxidative stress, inflammatory response, and the modulation of the cell proliferation due to the rich content of ω-3 PUFAs (Adeyemi and Olayaki, 2018; Baker et al., 2019; Shaaban et al., 2014; Wang et al., 2017). However, ω-3 PUFAs are facing low water-solubility, spontaneous oxidation, and deterioration during storage or the processing of food (Chang et al., 2018; Mohammed et al., 2020). These challenges may be resolved using several encapsulation technologies such as incorporating ω-3 PUFAs into the well-designed colloidal nanoparticles fabricated from the food ingredients, such as emulsion droplets, liposomes, microgels, or nanostructured lipid carriers to protect these them, control their release, and enhances their beneficial activities (Venugopalan et al., 2021). In the current study, animals that received EMFO in whey protein at the low or the high doses were compared with the control animals. The animals that received TiO_2-NPs plus EMFO showed a pronounced improvement in all the biochemical parameters, serum cytokines, the activity of antioxidant enzymes, genes expression, and the histological picture of the liver and kidney. This improvement in ALT and AST activity, TP, Alb, D BIL, and T. BIL reported herein in animals intoxicated with TiO_2-NPs plus EMFO agreed with the previous reports which indicated that ω-3 PUFAs reduce the activity of liver enzymes in various hepatic injury models (Yu et al., 2017). Additionally, the co-administration of EMFO and TiO_2-NPs resulted in a marked improvement in creatinine, uric acid, and urea. These results were in accordance with other reports which indicated that ω-3 PUFAs protect the kidney against different toxicants (Hassan and Gronert 2009; Moghadamnia et al., 2016). Moreover, EMFO also prevented the disturbances in lipid profile in animals that received TiO_2-NPs. These results also indicated that EMFO protected the liver and reduced its secretion of LDL (Wergedahl et al., 2009), modulate the cytochrome CYP7A1 expression, and activate the Cho catabolism to bile acid (Kim et al., 2012).

The present results also showed that EMFO prevented the reduction in these antioxidant enzymes (GPx, CAT, and SOD) in TiO_2-NPs-treated animals. In a previous study, Abdou and Hassan (2014) suggested that ω-3 PUFAs SH group in GSH from ROS besides it maintains the normal activity of CAT and SOD (Attia and Nasr, 2009) and up-regulate their corresponding gene expression (Khadke et al., 2020). Several reports suggesting that the mechanisms by which omega-3-rich fish oils include their ability to boost the production of GSH and the free radicals scavenging activity; therefore, they inhibit the peroxidation of lipids (Shaaban et al., 2014; Sohail et al., 2019). Moreover, it was reported that diet supplemented with ω-3 PUFAs increased cytochrome P450 2El (CYP2E1) content in the liver (Maksymchuk, 2014) with no significant changes in the lipid peroxidation or the balance between the hepatic prooxidant/antioxidant (Maksymchuk et al., 2015) Our results showed that EMFO diminished the increase of cytokines (AFP, TNF-α and CEA) levels in animals received TiO_2-NPs. In this concern, previous reports indicated that ω-3 PUFAs suppress the arachidonic acid transformation into the pro-inflammatory eicosanoids via different pathways including cyclooxygenase-2 and 5-lipoxygenase through inhibiting eicosanoid-generating enzymes activity or competing with the substrate in addition to the effect of their metabolites such as protectins and resolvins in hindering the steatosis and inflammation (El-Gendy et al., 2021; Wu et al., 2019). Moreover, ω-3 PUFAs were found to decrease the inflammation via the reduction of NF-kB concentration which in turn decreases the production of the inflammatory cytokines such as IL-1b and TNF-a beside the reduction of arachidonic acid-derived eicosanoids, consequently protect against the oxidative stress (Scorletti and Byrne, 2013). In addition, ω-3 PUFAs reduce the synthesis of inflammatory proteins which is probably mediated by altered activation of key transcription factors in the regulation of inflammatory gene expression including peroxisome proliferator-activated receptors and NF-kB (Calder, 2010).

The pathological alterations in the liver reported herein in the animals that received TiO_2-NPs included changes in the portal areas, dilatation with a thick wall of the portal vein, congestion, and periportal necrosis with proliferated bile ducts surrounded by aggregation of mononuclear cellular infiltration and fibrous tissues in the hepatic tissue. The kidney in this group also showed damaged tubules with pyknotic nuclei and cloudy swelling in the epithelial cells with segmentation and shrinkage of the glomeruli. These results were similar to those reported in our previous work (El-Nekeety et al., 2021). Co-administration of EMFO could reduce these histological changes in both organs. Similar observations were previously (Abdou and Hassan 2014; Abdel-Moneim et al., 2011).

5. Conclusion

This study revealed that 14 fatty acids were identified in Mullet fish oil included 41.4% PUFAs, 31,1% MUFAs, and 25.1% SFAs. The encapsulated mullet fish oil (EMFO) prepared using WPI showed a spherical structure with a mean diameter of 234.5 nm and ζ-potential of -6.24 mV was stable up to 10 days at 25 °C with EE of 81.08%. The PV of EMFO was decreased at 5 days then increased at 15 days; however, TBARS was increased by the storage time throughout 15 days. The biological evaluation of EMFO against the toxicity of TiO_2-NPs showed that exposure to TiO_2-NPs disturbs the biochemical parameters, lipid profile, inflammatory cytokines, oxidative stress markers, antioxidant enzymes, and their corresponding gene expression along with severe pathological changes in

the liver and kidney. Co-administration of EMFO induced a potent antioxidant property and diminished these disturbances and the high dose could normalize the majority of the parameters tested and the histology of the liver and kidney. Therefore, encapsulation of fish oil is a promising candidate for the protection of ω-3 PUFAs from oxidation and controls their release; hence, it can be applied in the food, medical applications and pharmaceutical industry.

6. Ethics approval

The investigation complies with the Guide for the Care and Use of Laboratory Animals published by the US National Institutes of Health (NIH Publication no. 85–23, revised 1996) and was approved by the Ethical Committee for Animal Experimentation at National Research Center. This article does not contain any studies with human participants.

Declarations

Author contribution statement

Mosaad A. Abdel-Wahhab: Conceived and designed the experiments; Analyzed and interpreted the data; Contributed reagents, materials, analysis tools or data; Wrote the paper.

Nabila S. Hassan; Sekena H. Abdel-Azieme; Aziza A. El-Nekeety; Hagar E. Mohammed; Tamer M. El-Messery; Mohamed H. Roby: Performed the experiments; contributed reagents, materials, analysis tools or data; Wrote the paper.

Funding statement

This work was supported by the National Research Centre, Dokki, Cairo, Egypt project #12050305.

Data availability statement

Data will be made available on request.

The authors are unable or have chosen not to specify which data has been used.

Declaration of interests statement

The authors declare no conflict of interest.

Additional information

No additional information is available for this paper.

References

Abdelhalim, M.A.K., Jarrar, B.M., 2011. The appearance of renal cells cytoplasmic degeneration and nuclear destruction might be an indication of GNPs toxicity. Lipids Health Dis. 10, 147.

Abdel-Moneim, A.E., Dkhil, M.A., Al-Quraishy, S., 2011. The redox status in rats treated with flaxseed oil and lead-induced hepatotoxicity. Biol. Trace Elem. Res. 143 (1), 457–467.

Abdel-Razek, A.G., Badr, A.N., El-Messery, T.M., El-Said, M.M., Hussein, A.M.S., 2018. Micro-nano encapsulation of Black seed oil ameliorate its characteristics and its mycotoxin inhibition. Biosci. Res. 15 (3), 2591–2601.

Abdel-Wahhab, M.A., El-Nekeety, A.A., Hassan, N.S., Gibriel, A.A., Abdel-Wahhab, K.G., 2018. Encapsulation of cinnamon essential oil in whey protein enhances the protective effect against single or combined sub-chronic toxicity of fumonisin B_1 and/or aflatoxin B_1 in rats. Environ. Sci. Pollu. Res. 25 (29), 29144–29161.

Abdel-Wahhab, M.A., El-Nekeety, A.A., Hathout, A.S., Salman, A.S., Abdel-Aziem, S.H., Hassan, N.S., Abdel-Aziz, M.S., 2020. Secondary metabolites from Bacillus sp. MERNA97 extract attenuates the oxidative stress, genotoxicity and cytotoxicity of aflatoxin B_1 in rats. Food Chem. Toxicol. 141, 111399.

Abdel-Wahhab, M.A., El-Nekeety, A.A., Mohammed, H.E., Elshafey, O.I., Abdel-Aziem, S.H., Hassan, N.S., 2021. Elimination of oxidative stress and genotoxicity of biosynthesized titanium dioxide nanoparticles in rats via supplementation with whey protein-coated thyme essential oil. Environ. Sci. Pollut. Res. Int.

Abdel-Wahhab, M.A., Hassan, M.A., El-Nekeety, A.A., Abdel-Aziem, S.H., Hassan, N.S., Jaswir, I., Salleh, H.M., 2021a. Zinc citrate loaded whey protein nanoparticles ameliorate CCl4-induced testicular injury via the regulation of Nrf2-Keap1 antioxidative signaling pathway. J. Drug Deliv. Sci. Technol. 61, 102322.

Abdou, H.M., Hassan, M.A., 2014. Protective role of omega-3 polyunsaturated fatty Acid against lead acetate-induced toxicity in liver and kidney of female rats BioMed. Res. Int. 2014. Article ID 435857, 11 pages.

Ackman, R.G., 1998. Remarks on official methods employing boron trifluoride in the preparation of methyl esters of the fatty acids of fish oils. J. Am. Oil Chem. Soc. 75, 541–545.

Adeyemi, W.J., Olayaki, L.A., 2018. Diclofenac-induced hepatotoxicity: low dose of omega-3 fatty acids have more protective effects. Toxicol. Rep. 5, 90–95.

Ammendolia, M.G., Iosi, F., Maranghi, F., Tassinari, R., Cubadda, F., Aureli, A., Raggi, F., Superti, A., Mantovani, B., 2017. De Berardis, Short-term oral exposure to low doses of nano-sized TiO_2 and potential modulatory effects on intestinal cells. Food Chem. Toxicol. 102, 63–75.

Ani, A., Ani, M., Moshtaghie, A.A., Ahmadvand, H., 2008. Changes in liver contents of lipid fractions following titanium exposure. Iran. J. Pharm. Res. (IJPR) 7 (3), 179–183.

Antoni, R., Johnston, K.L., Collins, A.L., Robertson, M.D., 2018. Intermittent v. continuous energy restriction: differential effects on postprandial glucose and lipid metabolism following matched weight loss in overweight/obese participants. Br. J. Nutr. 119 (5), 507–516.

Attia, A.M., Nasr, H.M., 2009. Dimethoate-induced changes in biochemical parameters of experimental rat serum and its neutralization by black seed (*Nigella sativa L.*) oil. Slovak J. Anim. Sci. 42 (2), 87–94.

Badr, A.N., El-Said, M.M., El-Messery, M.T., Abdel-Razek, A.G., 2019. Non-traditional oils encapsulation as novel food additive enhanced yoghurt safety against aflatoxins. Pakistan J. Biol. Sci. 22 (2), 51–58.

Bae, E.K., Lee, S.J., 2008. Microencapsulation of avocado oil by spray drying using whey protein and maltodextrin. J. Microencapsul. (8), 549–560.

Baker, M.A., Nandivada, P., Mitchell, P.D., Fell, G.L., Pan, A., Cho, B.S., De La Flor, D.J., Anez-Bustillos, L., Dao, D.T., Nosé, V., Puder, M., 2019. Omega-3 fatty acids are protective in hepatic ischemia reperfusion injury in the absence of GPR120 signaling. J. Pediatr. Surg. 54, 2392–2397.

Bancroft, D., Stevens, A., Turmer, R., 1996. Theory and Practice of Histological Technique, fourth ed. Churchill Livingstone, Edinburgh, pp. 36–42.

Baranowska-Wójcik, E., Szwajgier, D., Oleszczuk, P., Winiarska-Mieczan, A., 2020. Effects of titanium dioxide nanoparticles exposure on human health-a review. Biol. Trace Elem. Res. 193, 118–129.

Bouzidi, N., Mekki, k., Boukaddoum, A., Dida, N., Kaddous, A., Bouchenak, M., 2010. Effects of omega-3 polyunsaturated fatty-acid supplementation on redox status in chronic renal failure patients with dyslipidemia. J. Ren. Nutr. 20, 321–328.

Bratu, A., Mihaela, M., Hanganu, A., Chira, N.A., Todaşcă, M.C., Roşca, S., 2013. Quantitative determination of fatty acids from fish oils using GC-MS method and ^{1}H-NMR spectroscopy. U.P.B. Sci. Bull., Series B 75 (2), 23–32.

Brun, E., Barreau, F., Veronesi, G., Fayard, B., Sorieul, S., Chanéac, C., Carapito, C., Rabilloud, T., Mabondzo, A., Herlin-Boime, N., Carrière, M., 2014. Titanium dioxide nanoparticle impact and translocation through *ex vivo, in vivo* and *in vitro* gut epithelia. Part. Fibre Toxicol. 11, 2–16.

Bu, Q., Yan, G., Deng, P., Peng, F., Lin, H., Xu, Y., Cao, Z., Zhou, T., Xue, A., Wang, Y., Cen, X., Zhao, Y.L., 2010. NMR-based metabonomic study of the sub-acute toxicity of titanium dioxide nanoparticles in rats after oral administration. Nanotechnology 21 (12), 125105.

Calder, P.C., 2010. Omega-3 fatty acids and inflammatory processes. Nutrients 2, 355–374.

Calviello, G., Serini, S., Palozza, P., 2006. n-3 polyunsaturated fatty acids as signal transduction modulators and therapeutical agents in cancer. Curr. Signal Transduct. Ther. 1, 255–271.

Cansell, M., Nacka, F., Combe, N., 2003. Marine lipid-based liposomes increase *in vivo* FA bioavailability. Lipids 38 (5), 551–559.

Carneiro, H.C.F., Tonon, R.V., Grosso, C.R.F., Hubinger, M.D., 2013. Encapsulation efficiency and oxidative stability of flaxseed oil microencapsulated by spray drying using different combinations of wall materials. J. Food Eng. 115 (4), 443–451.

Carrepeiro, M.M., Rogero, M.M., Bertolami, M.C., Botelho, P.B., Castro, N., Castro, I.A., 2011. Effect of n-3 fatty acids and statins on oxidative stress in statin-treated hypercholestorelemic and normocholesterolemic women. Atherosclerosis 217, 171–178.

Chang, C., Nickerson, M.T., 2018. Encapsulation of omega 3-6-9 fatty acids-rich oils using protein-based emulsions with spray drying. J. Food Sci. Technol. 55 (8), 2850–2861.

Chen, J., Dong, X., Zhao, J., Tang, G., 2009. *In vivo* acute toxicity of titanium dioxide nanoparticles to mice after intraperitoneal injection. J. Appl. Toxicol. 29, 330–337.

Chen, Z., Han, S., Zheng, P., Zhou, D., Zhou, S., Jia, G., 2020. Effect of oral exposure to titanium dioxide nanoparticles on lipid metabolism in Sprague-Dawley rats. Nanoscale.

Chen, Z., Wang, Y., Zhuo, L., Chen, S., Zhao, L., Luan, X., Wang, H., Jia, G., 2015. Effect of titanium dioxide nanoparticles on the cardiovascular system after oral administration. Toxicol. Lett. 239 (2), 123–130.

Curioni, C., Alves, N., Zago, L., 2019. Omega-3 supplementation in the treatment of overweight and obese children and adolescents: a systematic review. J. Funct. Foods 52, 340–347.

Dambach, D.M., Andrews, B.A., Moulin, F., 2005. New technologies and screening strategies for hepatotoxicity: use of *in vitro* models. Toxicol. Pathol. 33 (1), 17–26.

Dawood, M.A.O., Koshio, S., Zaineldin, A.I., Van Doan, H., Moustafa, E.M., Abdel-Daim, M.M., Angeles, E.M., Hassaan, M.S., 2018. Dietary supplementation of

selenium nanoparticles modulated systemic and mucosal immune status and stress resistance of red sea bream (*Pagrus major*). Fish Physiol. Biochem. 45, 219–230.
Duan, Y., Liu, J., Ma, L., Li, N., Liu, H., Wang, J., Zheng, L., Liu, C., Wang, X., Zhao, X., Yan, J., Wang, S., Wang, H., Zhang, X., Hong, F., 2010. Toxicological characteristics of nanoparticulate anatase titanium dioxide in mice. Biomaterials 31 (5), 894–899.
El-Gendy, Z.A., El-Batran, S.A., Youssef, S., Ramadan, A., Hotaby, W.E., Bakeer, R.M., Ahmed, R.F., 2021. Hepatoprotective effect of Omega-3 PUFAs against acute paracetamol-induced hepatic injury confirmed by FTIR. Hum. Exp. Toxicol. 40 (3), 526–537.
Elias, R.J., Kellerby, S.S., Decker, E.A., 2008. Antioxidant activity of proteins and peptides. Crit. Rev. Food Sci. Nutr. 48, 430–441.
Ellulu, M.S., Khaza'ai, H., Abed, Y., Rahmat, A., Ismail, P., Ranneh, Y., 2015. Role of fish oil in human health and possible mechanism to reduce the inflammation. Inflammopharmacology 2379–2389.
El-Messery, T.M., Altuntas, U., Altin, G., Özçelik, B., 2020. The Effect of spray -drying and freeze-drying on encapsulation efficiency, in vitro bioaccessibility and oxidative stability of krill oil nanoemulsion system. Food Hydrocolloids 106, 105890.
El-Nekeety, A.A., Hassan, M.E., Hassan, R.R., Elshafey, O.I., Hamza, Z.K., Abdel-Aziem, S.H., Hassan, N.S., Abdel-Wahhab, M.A., 2021. Nanoencapsulation of basil essential oil alleviates the oxidative stress, genotoxicity and DNA damage in rats exposed to biosynthesized iron nanoparticles. Heliyon 7 (7), e07537.
Eltweri, A.M., Thomas, A.L., Metcalfe, M., Calder, P.C., Dennison, A.R., Bowrey, D.J., 2017. Potential applications of fish oils rich in omega-3 polyunsaturated fatty acids in the management of gastrointestinal cancer. Clin. Nutr. 36, 65–78.
Endo, J., Arita, M., 2016. Cardioprotective mechanism ofomega-3 polyunsaturated fatty acids. J. Cardiol. 67, 22–27.
Epstein, F.H., 1997. Oxygen and renal metabolism. Kidney Int. 51 (2), 381–385.
Estévez, M., 2015. Oxidative damage to poultry: from farm to fork. Poultr. Sci. 94 (6), 1368–1378.
Fartkhooni, F.M., Noori, A., Mohammadi, A., 2016. Effects of titanium dioxide nanoparticles toxicity on the kidney of male rats. Int. J. Life Sci. 10 (1), 65–69.
Federici, G., Shaw, B.J., Handy, R.D., 2007. Toxicity of titanium dioxide nanoparticles to rainbow trout (*Oncorhynchus mykiss*): gill injury, oxidative stress, and other physiological effects. Aquat. Toxicol. 84, 415–430.
Foroozandeh, P., Aziz, A.A., 2015. Merging worlds of nanomaterials and biological environment: factors governing protein corona formation on nanoparticles and its biological consequences. Nanoscale Res. Lett. 10, 221.
Goula, A.M., Adamopoulos, K.G., 2012. A method for pomegranate seed application in food industries: seed oil encapsulation. Food Bioprod. Process. 90 (4), 639–652.
Hassan, I.R., Gronert, K., 2009. Acute changes in dietary omega-3 and omega-6 polyunsaturated fatty acids have a pronounced impact on survival following ischemic renal injury and formation of renoprotective docosahexaenoic acid-derived protectin D1. J. Immunol. 182 (5), 3223–3232.
Hong, F., Zhou, Y., Zhao, X., Sheng, L., Wang, L., 2017. Maternal exposure to nanosized titanium dioxide suppresses embryonic development in mice. Int. J. Nanomed. 12, 6197–6204.
Horn, A.F., Nielsen, N.S., Jensen, L.S., Horsewell, A., Jacobsen, C., 2012. The choice of homogenisation equipment affects lipid oxidation in emulsions. Food Chem. 15, 803–810.
Hu, F.B., Bronner, L., Willer, W.C., 2002. Fish and omega-3 fatty acid intake and risk of coronary heart disease in women. JAMA 346, 1113–1118.
Hu, F.B., Cho, E., Rexrode, K.M., Albert, C.M., Manson, J.E., 2003. Fish and long-chain omega-3 fatty acid intake and risk of coronary heart disease and total mortality in diabetic women. Circulation 107 (14), 1852–1857.
Iavicoli, I., Leso, V., Fontana, I., Bergamaschi, A., 2011. Toxicological effects of titanium dioxide nanoparticles: a review of *in vitro* mammalian studies. Eur. Rev. Med. Pharmacol. Sci. 15, 481–508.
Ilani, M., Alaee, S., Khodabandeh, Z., Jamhiri, I., Owjfard, M., 2018. Effect of titanium dioxide nanoparticles on the expression of apoptotic markers in mouse blastocysts. Toxicol. Environ. Chem. 100 (2), 228–234.
Kandeil, M.A., Mohammed, E.T., Hashem, K.S., Aleya, L., Abdel-Daim, M.M., 2019. Moringa seed extract alleviates titanium oxide nanoparticles (TiO_2-NPs) induced cerebral oxidative damage and increases cerebral mitochondrial viability. Environ. Sci. Pollut. Res.
Kerdiles, O., Layé, S., Calon, F., 2017. Omega-3 polyunsaturated fatty acids and brain health: preclinical evidence for the prevention of neurodegenerative diseases. Trends Food Sci. Technol. 69, 203–213.
Khadke, S., Mandave, P., Kuvalekar, A., Pandit, V., Karandikar, M., Mantri, N., 2020. Synergistic effect of omega-3 fatty acids and oral-hypoglycemic drug on lipid normalization through modulation of hepatic gene expression in high fat diet with low streptozotocin-induced diabetic rats. Nutrients 12 (12), 3652.
Kim, E.H., Bae, J.S., Hahm, K.B., Cha, J.Y., 2012. Endogenously synthesized n- 3 polyunsaturated fatty acids in fat-1 mice ameliorate high-fat diet-induced non-alcoholic fatty liver disease. Biochem. Pharmacol. 84 (10), 1359–1365.
Kim, H.D., Shay, T., O'Shea, E.K., Regev, A., 2009. Transcriptional regulatorycircuits: predicting numbers from alphabets. Science (New York) 325 (5939), 429–432.
Kroemer, G., Galluzzi, L., Brenner, C., 2007. Mitochondrial membrane permeabilization in cell death. Physiol. Rev. 87, 99–163.
Kromhout, D., Bosschieter, E.B., de Lezenne Coulander, C., 1985. The inverse relation between fish consumption and 20-year mortality from coronary heart disease. N. Engl. J. Med. 312, 1205–1209.
Latchoumycandane, C., Mathur, P., 2002. Induction of oxidative stress in the rat testis after short-term exposure to the organochlorine pesticide methoxychlor. Arch. Toxicol. 76 (12), 692–698.
Li, Y., Yan, J., Ding, W., Chen, Y., Pack, L.M., Chen, T., 2017. Genotoxicity and gene expression analyses of liver and lung tissues of mice treated with titanium dioxide nanoparticles. Mutagenesis 32 (1), 33–46.
Lin, C.C., Hsu, Y.F., Lin, T.C., Hsu, F.L., Hsu, H.Y., 1998. Antioxidant and hepatoprotective activity of Punicalagin and Punicalin on carbon tetrachloride induced liver damage in rats. J. Pharm. Pharmacol. 50 (7), 789–794.
Maksymchuk, O., Shysh, A., Chashchyn, M., Moibenko, O., 2015. Dietary omega-3 polyunsaturated fatty acids alter fatty acid composition of lipids and CYP2E1 expression in rat liver tissue. Int. J. Vitam. Nutr. Res. 85, 322–328.
Maksymchuk, O.V., 2014. Influence of omega-3 polyunsaturated fatty acids on oxidative stress and cytochrome P450 2E1 expression in rat liver. Ukrainian Biochem. J. 86, 132–137.
McClements, D.J., Rao, J., 2011. Food-grade nanoemulsions: formulation, fabrication, properties, performance, biological fate, and potential toxicity. Crit. Rev. Food Sci. Nutr. 51, 285–330.
McClements, D.J., 2005. Principles, practice, and techniques. In: Food Emulsions, second ed. CRC Press, Boca Raton.
McClements, D.J., DeLoid, G., Pyrgiotakis, G., Shatkin, J.A., Xiao, H., Demokritou, P., 2016. The role of the food matrix and gastrointestinal tract in the assessment of biological properties of ingested engineered nanomaterials (iENMs): state of the science and knowledge gaps. NanoImpact 3, 47–57.
Migdal, C., Rahal, R., Rubod, A., Callejon, S., Colomb, E., Atrux-Tallau, N., Haftek, M., Vincent, C., Serres, M., Daniele, S., 2010. Internalisation of hybrid titanium dioxide/para-amino benzoic acid nanoparticles in human dendritic cells did not induce toxicity and changes in their functions. Toxicol. Lett. 199 (1), 34–42.
Moghadamnia, D., Mokhtar, M., Saeed, M.K., 2016. The Protective effect of omega-3 against thioacetamide induced lipid and renal dysfunction in male rats. Zahedan J. Res. Med. Sci. In Press.
Mohammed, E.T., Safwat, G.M., 2020. Grape seed proanthocyanidin extract mitigates titanium dioxide nanoparticle (TiO_2-NPs)-induced hepatotoxicity through TLR-4/NF-κB signaling pathway. Biol. Trace Elem. Res. 196, 579–589.
Mohammed, N.K., Tan, C.P., Manap, Y.A., Muhialdin, B.J., Hussin, A.S.M., 2020. Spray drying for the encapsulation of oils-A review. Molecules 25 (17), 3873. PMID: 32858785; PMCID: PMC7503953.
Moradi, A., Ziamajidi, N., Ghafourikhosroshahi, A., Abbasalipourkabir, R., 2019. Effects of vitamin A and vitamin E on attenuation of titanium dioxide nanoparticles-induced toxicity in the liver of male Wistar rats. Mol. Biol. Rep. 46, 2919–2932.
Morgan, A., Ibrahim, M.A., Galal, M.K., Ogaly, H.A., Abd-Elsalam, R.M., 2018. Innovative perception on using Tiron to modulate the hepatotoxicity induced by titanium dioxide nanoparticles in male rats. Biomed. Pharmacother. 103, 553–561.
Müller, L., Riediker, M., Wick, P., Mohr, M., Gehr, P., Rothen-rutishauser, B., 2010. Oxidative stress and inflammation response after nanoparticle exposure: differences between human lung cell monocultures and an advanced three-dimensional model of the human epithelial airways. J. R. Soc. Interface 7 (Suppl1), S27–S40.
Ningning, M., Qianru, G., Xiaoyu, L., Duoxia, X., Yingmao, Y., Yanping, C., 2020. Enhancing the physicochemical stability and digestibility of DHA emulsions by encapsulation of DHA droplets in caseinate/alginate honey comb shaped Microparticles. Food Funct. 11, 2080–2093.
Pandiangan, M., Kaban, J., Wirjosentono, B., Silalahi, J., 2018. Determination and identification of omega 3 and 6 fatty acids position in nile tilapia oil. IOP Conf. Ser. Earth Environ. Sci. 205 (2018), 012045.
Peng, X., Chen, K., Chen, J., Fang, J., Cui, H., Zuo, Z., Deng, J., Chen, Z., Geng, Y., Lai, W., 2016. Aflatoxin B_1 affects apoptosis and expression of Bax, Bcl-2, and Caspase-3 in thymus and bursa of fabricius in broiler chickens. Environ. Toxicol. 31 (9), 1113–1120.
Peters, R.J., van Bemmel, G., Herrera-Rivera, Z., Helsper, H.P., Marvin, H.J., Weigel, S., Tromp, P.C., Oomen, A.G., Rietveld, A.G., Bouwmeester, H., 2014. Characterization of titanium dioxide nanoparticles in food products: analytical methods to define nanoparticles. J. Agric. Food Chem. 62, 6285–6293.
Pfaffl, M.W., 2001. A new mathematical model for relative quantification in real-time RT-PCR. Nucleic Acids Res. 29 (900), 2002–2008.
Priscilla, D.H., Prince, P.S.M., 2009. Cardioprotective effect of gallic acid on cardiac troponin-T, cardiac marker enzymes, lipid peroxidation products and antioxidants in experimentally induced myocardial infarction in Wistar rats. Chem. Biol. Interact. 179 (2-3), 118–124.
Rajapakse, K., Drobne, D., Valant, J., Vodovnik, M., Levart, A., Marinsek-Logar, R., 2012. Acclimation of tetrahymena thermophila to bulk and nano-TiO_2 particles by changes in membrane fatty acids saturation. J. Hazard Mater. (221-222), 199–205.
Rajh, T., Dimitrijevic, N.M., Bissonnette, M., Koritarov, T., Konda, V., 2014. Titanium dioxide in the service of the biomedical revolution. Chem. Rev. 114 (19), 10177–10216.
Reeves, J.F., Davies, S.J., Dodd, N.J.F., Jha, A.N., 2008. Hydroxyl radicals (OH) are associated with titanium dioxide (TiO_2) nanoparticle-induced cytotoxicity and oxidative DNA damage in fish cells. Mutat. Res. Fund Mol. Mech. Mutagen 640, 113–122.
Reiner, Ž., 2017. Hypertriglyceridaemia and risk of coronary artery disease. Nat. Rev. Cardiol. 14 (7), 401–411.
Rikans, L.E., Hornbrook, K.R., 1997. Lipid peroxidation, antioxidant protection and aging. Biochim. Biophys. Acta (BBA) - Mol. Basis Dis. 1362, 116–127.
Saini, R.K., Keum, Y.S., 2018. Omega-3 and omega-6 polyunsaturated fatty acids: dietary sources, metabolism, and significance- A review. Life Sci. 203, 255–267.
Salman, A.S., Al-Shaikh, T.M., Hamza, Z.K., El-Nekeety, A.A., Bawazir, S.S., Hassan, N.S., Abdel-Wahhab, M.A., 2021. Matlodextrin-cinnamon essential oil nanoformulation as a potent protective against titanium nanoparticles-induced oxidative stress, genotoxicity, and reproductive disturbances in male mice. Environ. Sci. Pollut. Res. 2021.

Santonastaso, M., Mottola, F., Colacurci, N., Iovine, C., Pacifico, S.M., Cesaroni, F., Rocco, L., 2019. *In vitro* genotoxic effects of titanium dioxide nanoparticles (n-TiO_2) in human sperm cells. Mol. Reprod. Dev.

Scislowski, V., Bauchart, D., Gruffat, D., Laplaud, P., Durand, D., 2005. Effects of dietary n-6 or n-3 polyunsaturated fatty acids protected or not against ruminal hydrogenation on plasma lipids and their susceptibility to peroxidation in fattening steers 1. J. Anim. Sci. 83 (9), 2162–2174.

Scorletti, E., Byrne, C.D., 2013. Omega-3 fatty acids, hepatic lipid metabolism, and nonalcoholic fatty liver disease. Annu. Rev. Nutr. 33, 231–248.

Shaaban, A.A., Shaker, M.E., Zalata, K.R., El-kashef, H.A., Ibrahim, T.M., 2014. Modulation of carbon tetrachloride-induced hepatic oxidative stress, injury and fibrosis by olmesartan and omega-3. Chem. Biol. Interact. 207, 81–91.

Shakeel, M., Jabeen, F., Qureshi, N., Fakhr-e-Alam, M., 2016. Toxic effects of titanium dioxide nanoparticles and titanium dioxide bulk salt in the liver and blood of male Sprague-Dawley rats assessed by different assays. Biol. Trace Elem. Res. 173, 405–426.

Shakeel, M., Jabeen, F., Shabbir, S., Asghar, M.S., Khan, M.S., Chaudhry, A.S., 2016a. Toxicity of nano-titanium dioxide (TiO_2-NPs) through various routes of exposure: a review. Biol. Trace Elem. Res. 172, 1–36.

Sharma, P., Singh, R., Jan, M., 2014. Dose-dependent effect of deltamethrin in testis, liver, and kidney of Wistar rats. Toxicol. Int. 21 (2), 131–139.

Shi, Z., Niu, Y., Wang, Q., Shi, L., Guo, H., Liu, Y., Zhu, Y., Liu, S., Liu, C., Chen, X., Zhang, R., 2015. Reduction of DNA damage induced by titanium dioxide nanoparticles through Nrf2 *in vitro* and *in vivo*. J. Hazard Mater. 298, 310–319.

Shukla, R.K., Kumar, A., Vallabani, N.V.S., Pandey, A.K., Dhawan, A., 2014. Titanium dioxide nanoparticle-induced oxidative stress triggers DNA damage and hepatic injury in mice. Nanomedicine 9, 1423–1434.

Singh, H., 2011. Aspects of milk-protein-stabilised emulsions. Food Hydrocolloids 25, 1938–1944.

Skocaj, M., Filipic, M., Petkovic, J., Novak, S., 2011. Titanium dioxide in our everyday life; Is it safe? Radiol. Oncol. 45, 227–247.

Sohail, N., Hira, K., Tariq, A., Sultana, V., Ehteshamul-Haque, S., 2019. Marine macro-algae attenuates nephrotoxicity and hepatotoxicity induced by cisplatin and acetaminophen in rats. Environ. Sci. Pollut. Res. Int. 26, 25301–25311.

Thapa, B.R., Walia, A., 2007. Liver function tests and their interpretation. Indian J. Pediatr. 74 (7), 663–671.

Trouiller, B., Reliene, R., Westbrook, A., Solaimani, P., Schiestl, R.H., 2009. Titanium dioxide nanoparticles induce DNA damage and genetic instability in *vivo in* mice. Cancer Res. 69 (22), 8784–8789.

Valentini, X., Rugira, P., Frau, A., Tagliatti, V., Conotte, R., Laurent, S., Colet, J.M., Nonclercq, D., 2019. Hepatic and renal toxicity induced by TiO_2 nanoparticles in rats: a morphological and metabonomic study. J. Toxicol. 5767012, 19.

Venugopalan, V.K., Gopakumar, L.R., Kumaran, A.K., Chatterjee, N.S., Soman, V., Peeralil, S., Mathew, S., McClements, D.J., Nagarajarao, R.C., 2021. Encapsulation and protection of omega-3-rich fish oils using food-grade delivery systems. Foods 10 (7), 1566. PMID: 34359436; PMCID: PMC8305697.

Walker, R.M., Decker, E.A., Mcclements, D.J., 2015. Physical and oxidative stability of fish oil nanoemulsions produced by spontaneous emulsification: effect of surfactant concentration and particle size. J. Food Eng. 164, 10–20.

Wang, M., Zhang, X., Ma, L.J., Feng, R.B., Yan, C., Su, H., He, C., Kang, J.X., Liu, B., Wan, J.B., 2017. Omega-3 polyunsaturated fatty acids ameliorate ethanol-induced adipose hyperlipolysis: a mechanism for hepatoprotective effect against alcoholic liver disease. Biochim. Biophys. Acta (BBA) - Mol. Basis Dis. 1863, 3190–3201.

Weir, A., Westerhoff, P., Fabricius, L., von Goetz, N., 2012. Titanium dioxide nanoparticles in food and personal care products. Environ. Sci. Technol. 46, 2242–2250.

Wergedahl, H., Gudbrandsen, O.A., Rost, T.H., Berge, R.K., 2009. Combination of fish oil and fish protein hydrolysate reduces the plasma cholesterol level with a concurrent increase in hepatic cholesterol level in high-fat-fed Wistar rats. Nutrition 25 (1), 98–104.

Winkler, H.C., Notter, T., Meyer, U., Naegeli, H., 2018. Critical review of the safety assessment of titanium dioxide additives in food. J. Nanobiotechnol. 16 (1), 51.

Wu, C.T., Deng, J.S., Huang, W.C., Shieh, P.C., Chung, M.I., Huang, G.J., 2019. Salvianolic acid C against acetaminophen-induced acute liver injury by attenuating inflammation, oxidative stress, and apoptosis through inhibition of the Keap1/Nrf2/HO-1 signaling. Oxid. Med. Cell. Longev. 2019, 9056845.

Wu, T., Tang, M., 2018. The inflammatory response to silver and titanium dioxide nanoparticles in the central nervous system. Nanomedicine (London) 13 (2), 233–249.

Yang, Y.C., Lii, C.K., Wei, Y.L., Li, C.C., Lu, C.Y., Liu, K.L., Chen, H.W., 2013. Docosahexaenoic acid inhibition of inflammation is partially via cross-talk between Nrf2/heme oxygenase 1 and IKK/NF-κB pathways. J. Nutr. Biochem. 24, 204–212.

Yin, Z.F., Wu, L., Yang, H.G., Su, Y.H., 2013. Recent progress in biomedical applications of titanium dioxide. Phys. Chem. Chem. Phys. 15 (14), 4844–4858.

Yu, L., Yuan, M., Wang, L., 2017. The effect of omega-3 unsaturated fatty acids on non-alcoholic fatty liver disease: a systematic review and meta-analysis of RCTs. Pak. J. Med. Sci. 33, 1022–1028.

Zahin, N., Anwar, R., Tewari, D., Kabir, M.T., Sajid, A., Mathew, B., Uddin, M.S., Aleya, L., Abdel-Daim, M.M., 2020. Nanoparticles and its biomedical applications in health and diseases: special focus on drug delivery. Environ. Sci. Pollut. Res. Int. 16, 19151–19168.

Zhao, J., Bowman, L., Zhang, X., Vallyathan, V., Young, S.H., Castranova, V., Ding, M., 2009. Titanium dioxide (TiO2) nanoparticles induce JB6 Cell apoptosis through activation of the caspase-8/Bid and mitochondrial pathways. J. Toxicol. Environ. Health 72 (19), 1141–1149.